Explicit Solution of the Time Evolution of the Wigner Function†

Cheuk-Yin Wong

Physics Division, Oak Ridge National Laboratory, Oak Ridge, TN 37831-6373, USA

Abstract. Previously, an explicit solution for the time evolution of the Wigner function was presented in terms of auxiliary phase space coordinates which obey simple equations that are analogous with, but not identical to, the classical equations of motion. They can be solved easily and their solutions can be utilized to construct the time evolution of the Wigner function. In this paper, the usefulness of this explicit solution is demonstrated by solving a numerical example in which the Wigner function has strong spatial and temporal variations as well as regions with negative values. It is found that the explicit solution gives a correct description of the time evolution of the Wigner function. We examine next the pseudoparticle method which uses classical trajectories to evolve the Wigner function. We find that the lowest-order pseudoparticle approximation reproduces the general features of the time evolution, but there are deviations. We show how these deviations can be systematically reduced by including higher-order correction terms in powers of $\hbar^2$.

† Invited talk presented at the Wigner Centennial Conference, Pecs, Hungary, July 8-12, 2002, to be published in the Journal of Optics B: Quantum and Classical Optics, June 2003.

1. Introduction

It is a great pleasure for me to participate in the Wigner Centennial Conference at Pecs, Hungary in honor of the Centennial of Professor Eugene Wigner's birthday. I first met Professor Wigner in 1959 when I was an undergraduate student at Princeton. Professor Wigner taught us and our fellow graduate school classmates Curtis Callen, Stephen Adler, and Alfred Goldhaber a course in Advanced Quantum Mechanics in 1961. We were at the celebration party at the Graduate College when Professor Wigner was awarded the Nobel Prize in Physics in 1963. After I obtained my Ph. D. degree at Princeton, I came to work at Oak Ridge National Laboratory, for which Professor Wigner was the founding Scientific Director. I saw Professor Wigner from time to time at Oak Ridge when he came to work on his civil defense project. It is therefore particularly meaningful to me to come and celebrate his centennial in his native land to commemorate his many important contributions.

As a part of the "Junior Paper" research project at Princeton University, I went to see Professor Wigner in his office in Fine Hall in 1959 and inquired about the early history of Quantum Mechanics. He told me that the great thing about Schrödinger was that his wave equation was formulated in configuration space. However, to Professor Wigner, who was trained as a chemical engineer, dynamics could also be described in phase space. His formulation of quantum mechanics in phase space in 1932 led to the well-known Wigner description of quantum systems [1]. The joint function of coordinate and momentum $f(\boldsymbol{rp})$ introduced in 1932, now known as the Wigner function, is analogous with the classical distribution function. This analogy has provided new insights and useful applications to many quantum systems. It is deservedly a subject of intense interest in this Wigner Centennial Conference [2].

The Wigner function is, however, not identical to the classical distribution function. The classical distribution function is always non-negative and can be described in terms of a collection of cell points with positive weights in phase space. The evolution of the classical distribution function can be followed by tracking these cell points using classical equations of motion [3].

The Wigner function can assume negative as well as positive values in some regions of phase space. How does a Wigner function with regions of negative values evolve as a function of time? The concept of a probability distribution function with positive weights is clearly not applicable here. The difficulty of propagating the Wigner function with negative values has been a barrier to the study of the dynamics of the Wigner function using the equation of motion of the Wigner function directly.

Previously, I formulated a simple method to propagate the Wigner function in time [3]. The ability to propagate the Wigner function with negative values arises from the fact that one deals with amplitudes in this method, and one does not need to use the concept of probabilities. The method contains three important components. First, one employs an auxiliary variable $\boldsymbol{s}$, which is allowed to span the whole configuration space. Second, using this auxiliary variable $\boldsymbol{s}$, the Wigner function can be represented

in terms of auxiliary phase space coordinates $\boldsymbol{R}$ and $\boldsymbol{P}$. The equations of motion for these auxiliary coordinates $\boldsymbol{R}$ and $\boldsymbol{P}$ are quite simple. They are analogous with, but not identical to, the classical equations of motion, as $\partial \boldsymbol{P}/\partial t$ depends on the auxiliary coordinate $\boldsymbol{s}$. They can be solved easily and their solutions can be utilized to construct the Wigner function at the next time step. The third component consists of providing the correct amplitude function for the evolution. For each value of $\boldsymbol{s}$ and the evolution of phase space coordinates, one associates an amplitude factor $\exp\{i\boldsymbol{s}\cdot(\boldsymbol{p}-\boldsymbol{P})/\hbar\}$. After the amplitudes for all possible values of $\boldsymbol{s}$ have been obtained at the end of one time step, one adds all these amplitudes together coherently (Huygen Principle) to give the Wigner function $f(\boldsymbol{rp})$ at the next time step. This explicit solution overcomes the difficulty of propagating a Wigner function with negative values.

Recently, with the rapid advances in quantum information technology and the reduction in the size of micro-electronic devices, there has been renewed interest in experimental and theoretical studies of the Wigner function [4]-[20]. Experimental measurements of the Wigner function have been carried out using many different techniques [4]-[9]. Regions of negative Wigner function were observed in many experiments [5, 8]. The time evolution of the Wigner function has been studied by many authors [10]−[24]. It is instructive to review the explicit solution for the time evolution of the Wigner function obtained previously and to demonstrate its usefulness by a numerical example. We choose to examine an example in which the time evolution of the Wigner function can be ready evaluated by using wave functions and eigenvalues. The Wigner function in the example should have significant spatial and temporal variations as well as regions of negative values to test whether the explicit solution obtained previously is capable of treating these non-classical features. The success in providing a correct time evolution of the Wigner function using this explicit solution will pave the way for its applications in the future.

As an approximation of the explicit solution, a pseudoparticle method was developed previously [3] to obtain the time evolution of the Wigner function by following the trajectories of the phase space coordinates, using classical equations of motion . It is instructive to review this pseudoparticle method and assess its accuracy by comparing with the correct results. Furthermore, it is useful to develop systematic ways to improve the accuracy of the pseudoparticle method to assist its future applications.

2. Explicit Solution of the Time Evolution of the Wigner Function

We shall first review the explicit solution obtained in 1982 [3]. We consider a particle in the potential V

$$i\hbar\frac{\partial}{\partial t}\psi(\boldsymbol{r},t)=\left\{-\frac{\hbar^2}{2m}\nabla^2+V(\boldsymbol{r},t)\right\}\psi(\boldsymbol{r},t). \tag{1}$$

The Wigner function is

$$f(\boldsymbol{rp},t)=\int d\boldsymbol{s}\, e^{i\boldsymbol{p}\cdot\boldsymbol{s}/\hbar}\psi(\boldsymbol{r}-\frac{\boldsymbol{s}}{2},t)\psi^*(\boldsymbol{r}+\frac{\boldsymbol{s}}{2},t). \tag{2}$$

From the Schrödinger equation, we obtain the equation of motion for the Wigner function [1]

$$\frac{\partial f(\boldsymbol{rp},t)}{dt}+\frac{\boldsymbol{p}}{m}\cdot\nabla_r f(\boldsymbol{rp},t)-\frac{2}{\hbar}\sin\left\{\frac{\hbar}{2}\nabla_r^V\cdot\nabla_p^f\right\}V(\boldsymbol{r},t)f(\boldsymbol{rp},t)=0, \quad (3)$$

where ∇_r^V acts on the potential V and ∇_p^f acts on the Wigner function f.

Given the Wigner function $f(\boldsymbol{r}_0\boldsymbol{p}_0,t_0)$ at time t_0, we wish to obtain the Wigner function at the next time step at $t=t_0+\delta t$ with a small δt. To solve for the dynamics, we divide the phase space into cells (pseudoparticles). Consider one such cell centered at $\{\boldsymbol{r}_0\ \boldsymbol{p}_0\}$ at time t_0 with volume element $d\boldsymbol{r}_0d\boldsymbol{p}_0$ and amplitude $f(\boldsymbol{r}_0\boldsymbol{p}_0,t_0)$. We retain the auxiliary coordinate $\boldsymbol{s}$ and follow the time dependence of each cell in the Lagrangian sense. For the phase space coordinates $\{\boldsymbol{r}_0\boldsymbol{p}_0\}$ initially at time t_0, we label their phase space coordinates at subsequent time t by $\{\boldsymbol{R}(\boldsymbol{r}_0\boldsymbol{p}_0\boldsymbol{s},t)\ \boldsymbol{P}(\boldsymbol{r}_0\boldsymbol{p}_0\boldsymbol{s},t)\}$. In classical dynamics, the evolution of the phase space coordinates will not depend on $\boldsymbol{s}$. In quantum dynamics, they will depend on $\boldsymbol{s}$. The momentum coordinate $\boldsymbol{P}$ can jump to the momentum coordinate $\boldsymbol{p}$ at time t. We associate an amplitude of $\exp\{i\boldsymbol{s}\cdot[\boldsymbol{p}-\boldsymbol{P}(\boldsymbol{r}_0\boldsymbol{p}_0\boldsymbol{s},t)]/\hbar\}$ for this momentum jump. This amplitude factor is chosen because for the classical case where $\boldsymbol{P}$ is independent of $\boldsymbol{s}$ this amplitude leads to the correct delta function propagator $\delta(\boldsymbol{p}-\boldsymbol{P}(\boldsymbol{r_0p_0},\boldsymbol{t}))$ after we integrate over $\boldsymbol{s}$ [see Eq. (14)]. We therefore express the Wigner function $f(\boldsymbol{rp},t)$ at the next time step as [3]

$$f(\boldsymbol{rp},t)=\int\frac{d\boldsymbol{r}_0d\boldsymbol{p}_0d\boldsymbol{s}}{(2\pi\hbar)^3}\exp\{i\boldsymbol{s}\cdot[\boldsymbol{p}-\boldsymbol{P}(\boldsymbol{r}_0\boldsymbol{p}_0\boldsymbol{s},t)]/\hbar\}\delta[\boldsymbol{r}-\boldsymbol{R}(\boldsymbol{r}_0\boldsymbol{p}_0\boldsymbol{s},t)]f(\boldsymbol{r}_0\boldsymbol{p}_0,t_0). \quad (4)$$

Our task is to find solutions for the phase space coordinates $\boldsymbol{R}(\boldsymbol{r}_0\boldsymbol{p}_0\boldsymbol{s},t)$ and $\boldsymbol{P}(\boldsymbol{r}_0\boldsymbol{p}_0\boldsymbol{s},t)$ with initial conditions $\boldsymbol{R}(\boldsymbol{r}_0\boldsymbol{p}_0\boldsymbol{s},t_0)=\boldsymbol{r}_0$ and $\boldsymbol{P}(\boldsymbol{r}_0\boldsymbol{p}_0\boldsymbol{s},t_0)=\boldsymbol{p}_0$. If we can find these coordinates at the next time step, the above integral can then be carried out to give the Wigner function at the new time t.

To obtain the equations of motion for $\boldsymbol{R}(\boldsymbol{r}_0\boldsymbol{p}_0\boldsymbol{s},t)$ and $\boldsymbol{P}(\boldsymbol{r}_0\boldsymbol{p}_0\boldsymbol{s},t)$, we substitute Eq. (4) into Eq. (3). For the first term in Eq. (3), we get

$$\begin{aligned}\frac{\partial f(\boldsymbol{rp},t)}{\partial t}&=\int\frac{d\boldsymbol{r}_0d\boldsymbol{p}_0d\boldsymbol{s}}{(2\pi\hbar)^3}f(\boldsymbol{r}_0\boldsymbol{p}_0,t_0)\\&\times\left[\frac{(-i\boldsymbol{s})}{\hbar}\cdot\frac{\partial\boldsymbol{P}}{\partial t}\exp\{i\boldsymbol{s}\cdot[\boldsymbol{p}-\boldsymbol{P}(\boldsymbol{r}_0\boldsymbol{p}_0\boldsymbol{s},t)]/\hbar\}\delta[\boldsymbol{r}-\boldsymbol{R}(\boldsymbol{r}_0\boldsymbol{p}_0\boldsymbol{s},t)]\right.\\&\left.+\exp\{i\boldsymbol{s}\cdot[\boldsymbol{p}-\boldsymbol{P}(\boldsymbol{r}_0\boldsymbol{p}_0\boldsymbol{s},t)]/\hbar\}(\nabla_{\boldsymbol{R}}\delta[\boldsymbol{r}-\boldsymbol{R}(\boldsymbol{r}_0\boldsymbol{p}_0\boldsymbol{s},t)])\cdot\partial\boldsymbol{R}(\boldsymbol{r}_0\boldsymbol{p}_0\boldsymbol{s},t)/\partial t\right]. \quad (5)\end{aligned}$$

Noting that

$$\nabla_{\boldsymbol{R}}\delta[\boldsymbol{r}-\boldsymbol{R}(\boldsymbol{r}_0\boldsymbol{p}_0\boldsymbol{s},t)]=-\nabla_{\boldsymbol{r}}\delta[\boldsymbol{r}-\boldsymbol{R}(\boldsymbol{r}_0\boldsymbol{p}_0\boldsymbol{s},t)], \quad (6)$$

we can rewrite the second term inside the square bracket as

$$\begin{aligned}&\int\frac{d\boldsymbol{r}_0d\boldsymbol{p}_0d\boldsymbol{s}}{(2\pi\hbar)^3}f(\boldsymbol{r}_0\boldsymbol{p}_0,t_0)\\&\times\exp\{i\boldsymbol{s}\cdot[\boldsymbol{p}-\boldsymbol{P}(\boldsymbol{r}_0\boldsymbol{p}_0\boldsymbol{s},t)]/\hbar\}(-\nabla_{\boldsymbol{r}}\delta[\boldsymbol{r}-\boldsymbol{R}(\boldsymbol{r}_0\boldsymbol{p}_0\boldsymbol{s},t)]\cdot\partial\boldsymbol{R}(\boldsymbol{r}_0\boldsymbol{p}_0\boldsymbol{s},t)/\partial t\\&=-\frac{\partial\boldsymbol{R}(\boldsymbol{r}_0\boldsymbol{p}_0\boldsymbol{s},t)}{\partial t}\cdot\nabla_{\boldsymbol{r}}f(\boldsymbol{rp},t), \quad (7)\end{aligned}$$

where we have used Eq. (4) to obtain the right-hand side. For the last term in Eq. (3), we substitute (4) into this term and find

$$\frac{2}{\hbar}\sin\left\{\frac{\hbar}{2}\nabla_r^V\cdot\nabla_p^f\right\}V(\boldsymbol{r},t)f(\boldsymbol{rp},t)=\frac{1}{\hbar}\int\frac{d\boldsymbol{r}_0d\boldsymbol{p}_0d\boldsymbol{s}}{(2\pi\hbar)^3}f(\boldsymbol{r}_0\boldsymbol{p}_0,t_0)$$
$$\times\exp\{i\boldsymbol{s}\cdot[\boldsymbol{p}-\boldsymbol{P}(\boldsymbol{r}_0\boldsymbol{p}_0\boldsymbol{s},t)]/\hbar\}\delta[\boldsymbol{r}-\boldsymbol{R}(\boldsymbol{r}_0\boldsymbol{p}_0\boldsymbol{s},t)])\frac{[V(\boldsymbol{r}-\frac{\boldsymbol{s}}{2},t)-V(\boldsymbol{r}+\frac{\boldsymbol{s}}{2},t)]}{i}. \quad (8)$$

Putting Eqs. (5)-(8) into Eq. (3), we obtain

$$\left[-\frac{\partial\boldsymbol{R}(\boldsymbol{r}_0\boldsymbol{p}_0\boldsymbol{s},t)}{\partial t}+\frac{\boldsymbol{p}}{m}\right]\cdot\nabla_r f(\boldsymbol{rp},t)$$
$$+\int\frac{d\boldsymbol{r}_0d\boldsymbol{p}_0d\boldsymbol{s}}{(2\pi\hbar)^3}f(\boldsymbol{r}_0\boldsymbol{p}_0,t_0)\left[\frac{(-i\boldsymbol{s})}{\hbar}\cdot\frac{\partial\boldsymbol{P}}{\partial t}-\frac{[V(\boldsymbol{r}-\frac{\boldsymbol{s}}{2},t)-V(\boldsymbol{r}+\frac{\boldsymbol{s}}{2},t)]}{i\hbar}\right]$$
$$\times\exp\{i\boldsymbol{s}\cdot[\boldsymbol{p}-\boldsymbol{P}(\boldsymbol{r}_0\boldsymbol{p}_0\boldsymbol{s},t)]/\hbar\}\delta[\boldsymbol{r}-\boldsymbol{R}(\boldsymbol{r}_0\boldsymbol{p}_0\boldsymbol{s},t)]=0. \quad (9)$$

By comparing similar terms, the above equation leads to the equations of motion for $\boldsymbol{R}$ and $\boldsymbol{P}$ [3],

$$\frac{\partial\boldsymbol{R}}{\partial t}=\frac{\boldsymbol{p}}{m}, \quad (10)$$

$$\boldsymbol{s}\cdot\frac{\partial\boldsymbol{P}}{\partial t}=V\left(\boldsymbol{R}-\frac{\boldsymbol{s}}{2},t\right)-V\left(\boldsymbol{R}+\frac{\boldsymbol{s}}{2},t\right). \quad (11)$$

In the above equations, $\boldsymbol{r}$ and $\boldsymbol{R}$ are interchangeable, because of the δ-function $\delta(\boldsymbol{r}-\boldsymbol{R})$ in Eq. (4). It is interesting to note that these two equations were used recently by Morawetz to study the quantum response of a finite fermion system [19].

Equation (4) combined with the equations of motion (10) and (11) gives an explicit and exact solution of the time evolution of the Wigner function [3]. The equation of motion for $\boldsymbol{R}$ is the same as the classical equation of motion. The equation of motion for $\boldsymbol{P}$ coincides with the classical equation of motion for small $\boldsymbol{s}$ but differs from the classical equation when $\boldsymbol{s}$ is large. The latter difference distinguishes a quantum system from a classical system.

We note that if (1) we expand Eq. (11) in $\boldsymbol{s}$ and we keep only the lowest order term, or if (2) we take the limit $\hbar\to 0$ so that the dominant contributions in Eq. (4) come from regions of small $\boldsymbol{s}$, then Eqs. (10) and (11) becomes the classical equations of motion [3]

$$\frac{\partial\boldsymbol{R}}{\partial t}=\frac{\boldsymbol{p}}{m} \quad (12)$$

and

$$\frac{\partial\boldsymbol{P}}{\partial t}=-\nabla_R V(R,t). \quad (13)$$

The function $\boldsymbol{P}(\boldsymbol{r}_0\boldsymbol{p}_0\boldsymbol{s},t)$ is then independent of $\boldsymbol{s}$, and Eq. (4) gives

$$f(\boldsymbol{rp},t)=\int d\boldsymbol{r}_0d\boldsymbol{p}_0\delta[\boldsymbol{r}-\boldsymbol{R}(\boldsymbol{r}_0\boldsymbol{p}_0,t)]\delta[\boldsymbol{p}-\boldsymbol{P}(\boldsymbol{r}_0\boldsymbol{p}_0,t)]f(\boldsymbol{r}_0\boldsymbol{p}_0,t_0), \quad (14)$$

which is the same as solution of the evolution of the classical distribution function.

3. Implementation of the Explicit Solution

The explicit solution of Eqs. (4), (10) and (11) given in the previous section allows one to propagate the Wigner function from one time to another. One considers a small time increment $\delta t = t - t_0$, and solves Eqs. (10) and (11). One obtains

$$\boldsymbol{r} = \boldsymbol{R}(\boldsymbol{r}_0\boldsymbol{p}_0\boldsymbol{s}, t) = \boldsymbol{r}_0 + \frac{\boldsymbol{p}}{m}\delta t. \tag{15}$$

and

$$\boldsymbol{P} = \boldsymbol{p}_0 + \boldsymbol{e}_s \frac{V\left(\boldsymbol{r} - \frac{\boldsymbol{s}}{2}, t\right) - V\left(\boldsymbol{r} + \frac{\boldsymbol{s}}{2}, t\right)}{s}\ \delta t, \tag{16}$$

where $\boldsymbol{e}_s$ is the unit vector in the $\boldsymbol{s}$ direction. After $\boldsymbol{r}(\boldsymbol{R})$ and $\boldsymbol{P}$ for different $\boldsymbol{s}$ have been obtained, we can substitute them in Eq. (4) and carry out the integration to give the new Wigner function at the next time step. Eqs. (15) and (16) lead to

$$f(\boldsymbol{r}\boldsymbol{p}, t) = \int d\boldsymbol{r}_0 d\boldsymbol{p}_0 \int \frac{d\boldsymbol{s}}{(2\pi\hbar)^3} \exp\left[i\left\{\frac{\boldsymbol{s}\cdot(\boldsymbol{p}-\boldsymbol{p}_0)}{\hbar} - \left(V(\boldsymbol{r} - \frac{\boldsymbol{s}}{2}, t) - V(\boldsymbol{r} + \frac{\boldsymbol{s}}{2}, t)\right)\frac{\delta t}{\hbar}\right\}\right]$$
$$\times\delta(\boldsymbol{r} - \boldsymbol{r}_0 - \frac{\boldsymbol{p}}{m}\delta t) f(\boldsymbol{r}_0, \boldsymbol{p}_0, t_0). \tag{17}$$

We shall first consider the one-dimensional case for which the factor $(2\pi\hbar)^3$ becomes $2\pi\hbar$. The integration over $x_0(\boldsymbol{r}_0)$ can be easily carried out. the above equation for the one-dimensional case becomes

$$f(xp, t) = \int dp_0\ 2\int_0^\infty \frac{ds}{2\pi\hbar} \cos\left[\frac{s\cdot(p-p_0)}{\hbar} - \left(V(x - \frac{s}{2}, t) - V(x + \frac{s}{2}, t)\right)\frac{\delta t}{\hbar}\right]$$
$$\times f(x - \frac{p}{m}\delta t, p_0, t_0). \tag{18}$$

This explicit solution of the time evolution of the Wigner function can be written as

$$f(xp, t) = \int dp_0 \Big\{F_c(x, p-p_0) + F_s(x, p-p_0)\Big\} f(x - \frac{p}{m}\delta t, p_0, t_0), \tag{19}$$

where $F_c(x, p-p_0)$ and $F_s(x, p-p_0)$ are cosine and sine transforms given by

$$F_c(x, p-p_0) = 2\int_0^\infty \frac{ds}{2\pi\hbar} \cos\left[\frac{s\cdot(p-p_0)}{\hbar}\right] \cos\Big[\Big(V(x - \frac{s}{2}, t) - V(x + \frac{s}{2}, t)\Big)\frac{\delta t}{\hbar}\Big] \tag{20}$$

and

$$F_s(x, p-p_0) = 2\int_0^\infty \frac{ds}{2\pi\hbar} \sin\left[\frac{s\cdot(p-p_0)}{\hbar}\right] \sin\Big[\Big(V(x - \frac{s}{2}, t) - V(x + \frac{s}{2}, t)\Big)\frac{\delta t}{\hbar}\Big]. \tag{21}$$

The above set of equations (19)-(21) provide a simple implementation of the explicit solution (4), (11), and (10) of the time evolution of a one-dimensional Wigner function.

If one keeps only terms up to first order in δt for small values of δt, the Wigner function evolution equation becomes

$$f(xp, t) = f(x - \frac{p}{m}\delta t, p, t_0) + \frac{\delta t}{\hbar}\int dp_0 V_s(x, p-p_0) f(x - \frac{p}{m}\delta t, p_0, t_0), \tag{22}$$

where

$$V_s(x, p-p_0) = 2\int_0^\infty \frac{ds}{(2\pi\hbar)^3} \sin\left[\frac{s\cdot(p-p_0)}{\hbar}\right] \Big\{V(x - \frac{s}{2}, t) - V(x + \frac{s}{2}, t)\Big\}. \tag{23}$$

We shall now discuss the three-dimensional case for which the integration over $\boldsymbol{s}$ in Eq. (17) is rather complicated. It can be simplified if one makes the following approximation

$$V(\boldsymbol{r}-\frac{\boldsymbol{s}}{2},t)-V(\boldsymbol{r}+\frac{\boldsymbol{s}}{2},t)\approx\sum_{j=1}^{3}\Big(V(\boldsymbol{r}-\frac{s_j\boldsymbol{e}_j}{2},t)-V(\boldsymbol{r}+\frac{s_j\boldsymbol{e}_j}{2},t)\Big), \quad (24)$$

where the righthand side contains all terms of the lefthand side except the cross terms involving products of different s_j and $s_{j'}(j'\neq j)$ with high-order derivatives of $V(\boldsymbol{r})$, when one expand the above functions in powers of s_j. If one uses this approximation by neglecting these cross terms, Eq. (17) for the three-dimensional case becomes

$$f(\boldsymbol{r}\boldsymbol{p},t)=\int d\boldsymbol{p}_0\prod_{j=1}^{3}\ 2\int_0^\infty\frac{ds_j}{2\pi\hbar}\cos\left[\frac{s_j(p_j-p_{0j})}{\hbar}-\Big(V(\boldsymbol{r}-\frac{s_j\boldsymbol{e}_j}{2},t)-V(\boldsymbol{r}+\frac{s_j\boldsymbol{e}_j}{2},t)\Big)\frac{\delta t}{\hbar}\right]$$
$$\times f(\boldsymbol{r}-\frac{\boldsymbol{p}}{m}\delta t,\boldsymbol{p}_0,t_0). \quad (25)$$

The explicit solution of the time evolution of the Wigner function can be written as

$$f(\boldsymbol{r}\boldsymbol{p},t)=\int d\boldsymbol{p}_0\prod_{j=1}^{3}\Big\{F_{cj}(\boldsymbol{r},p_j-p_{0j})+F_{sj}(\boldsymbol{r},p_j-p_{0j})\Big\}f(\boldsymbol{r}-\frac{\boldsymbol{p}}{m}\delta t,\boldsymbol{p}_0,t_0), \quad (26)$$

where $F_{cj}(\boldsymbol{r},p_j-p_{0j})$ and $F_{sj}(\boldsymbol{r},p_j-p_{0j})$ are cosine and sine transforms given by

$$F_{cj}(\boldsymbol{r},p_j-p_{0j})=2\int_0^\infty\frac{ds_j}{2\pi\hbar}\cos\left[\frac{s_j(p_j-p_{0j})}{\hbar}\right]\cos\Big[\Big(V(\boldsymbol{r}-\frac{s_j\boldsymbol{e}_j}{2},t)-V(\boldsymbol{r}+\frac{s_j\boldsymbol{e}_j}{2},t)\Big)\frac{\delta t}{\hbar}\Big] \quad (27)$$

and

$$F_{sj}(\boldsymbol{r},p_j-p_{0j})=2\int_0^\infty\frac{ds_j}{2\pi\hbar}\sin\left[\frac{s_j(p_j-p_{0j})}{\hbar}\right]\sin\Big[\Big(V(\boldsymbol{r}-\frac{s_j\boldsymbol{e}_j}{2},t)-V(\boldsymbol{r}+\frac{s_j\boldsymbol{e}_j}{2},t)\Big)\frac{\delta t}{\hbar}\Big]. \quad (28)$$

The above set of equations (26)-(28) provide a simple and approximate implementation of the explicit solution (4), (11), and (10) of the time evolution of a three-dimensional Wigner function.

4. An Example of the Evolution of the Wigner Function

It is of interest to consider an explicit example to test whether the solutions in Eqs. (19)-(21) or (22)-(23) leads to the correct results. For this purpose we study the dynamics of the Wigner function for a case that can be easily evaluated and compared with the Wigner function obtained by using the explicit solution.

We examine a particle in a one-dimensional attractive Gaussian potential well. We express physical quantities in dimensionless units, with a Schrödinger equation given by

$$H\Psi(x)=\left\{-\frac{1}{2}\frac{d^2}{dx^2}-e^{-x^2/2\sigma^2}\right\}\Psi(x). \quad (29)$$

The wave function $\Psi(x)$ can be expanded in terms of a set of non-orthogonal Gaussian wave functions with different widths,

$$\Psi(x) = \sum_{n=1}^{n_{\max}} a_n \psi_n(x), \tag{30}$$

where the normalized basis function $\langle x|n\rangle = \psi_n(x)$ is taken to be

$$\psi_n(x) = \frac{e^{-x^2/2\beta_n^2}}{(\sqrt{\pi}\beta_n)^{1/2}}, \tag{31}$$

and $\beta_n^2 = n\beta_0^2$. The Hamiltonian matrix in this basis set can be easily constructed. Specifically, one calculates the matrix element of the overlap matrix B for this set of basis states

$$B_{nm} = \langle n|m\rangle = \sqrt{\frac{2\beta_n\beta_m}{\beta_n^2+\beta_m^2}}, \tag{32}$$

the matrix element of the kinetic energy matrix T

$$T_{nm} = \langle n| \left\{ -\frac{1}{2}\frac{d^2}{dx^2} \right\} |m\rangle = \frac{1}{2}\sqrt{\frac{2\beta_n\beta_m}{\beta_n^2+\beta_m^2}}\frac{1}{\beta_n^2+\beta_m^2}\ , \tag{33}$$

and the matrix element for potential energy matrix V

$$V_{nm} = \langle n|(-e^{-x^2/2\sigma^2})|m\rangle = -\sqrt{\frac{2\beta_n\beta_m}{\beta_n^2+\beta_m^2}\frac{\sigma^2}{\beta_{nm}^2+\sigma^2}}\ , \tag{34}$$

where

$$\beta_{nm}^2 = \frac{\beta_n^2\beta_m^2}{\beta_n^2+\beta_m^2}. \tag{35}$$

The eigenvalue equation becomes

$$(T+V)a = EBa, \tag{36}$$

where a is the column matrix of the coefficients $\{a_n\}$ of Eq. (30). This eigenvalue equation can be diagonalized to yield the eigenenergies E_λ and eigenfunctions $\Psi_\lambda(x)$ represented by the set of coefficients $\{a_{\lambda n}\}$. We normalize $\Psi_\lambda(x)$ by $\int dx|\Psi_\lambda(x)|^2 = 1$.

A simple non-stationary state $\Phi(x)$ of the system can be constructed as a linear combination of the eigenstates $\Psi_\lambda(x)$ with amplitudes b_λ,

$$\Phi(x, t=0) = \sum_\lambda b_\lambda \Psi_\lambda(x). \tag{37}$$

The time dependence of this non-stationary system is

$$\Phi(x,t) = \sum_\lambda b_\lambda e^{-iE_\lambda t}\Psi_\lambda(x). \tag{38}$$

The Wigner function of the system is then given by

$$f(xp,t) = \sum_{nm} c_n(t)c_m^*(t)f_{nm}(xp), \tag{39}$$

where

$$c_n(t) = \sum_\lambda b_\lambda e^{-iE_\lambda t}a_{\lambda n}, \tag{40}$$

$$f_{nm}(xp) = 2\sqrt{\frac{2\beta_n\beta_m}{\beta_n^2+\beta_m^2}}e^{-\nu_{nm}}, \tag{41}$$

$$\nu_{nm} = \frac{(\beta_n^2+\beta_m^2)(x^2-\mu_{nm}^2/4)}{2\beta_n^2\beta_m^2}, \tag{42}$$

and

$$\mu_{nm} = 4\frac{\beta_n^2\beta_m^2}{\beta_n^2+\beta_m^2}\left[x\left(\frac{1}{2\beta_n^2}-\frac{1}{2\beta_m^2}\right)+ip\right] \ . \tag{43}$$

In our numerical example, we study the dynamics of a system in a potential with a width parameter $\sigma = 3$. The two lowest energy even-parity eigenstates $\Psi_0(x)$ and $\Psi_1(x)$ have eigenvalues $E_0 = -0.844$ and $E_1 = -0.312$ respectively. As a test, we construct a non-stationary wave function with equal amplitudes in these two eigenstates at $t = 0$,

$$\Phi(x, t=0) = \frac{1}{\sqrt{2}}\{\Psi_0(x)+\Psi_1(x)\}. \tag{44}$$

The time dependence of the wave function is then

$$\Phi(x,t) = \frac{1}{\sqrt{2}}\{e^{-iE_0t}\Psi_0(x)+e^{-iE_1t}\Psi_1(x)\}. \tag{45}$$

The time dependence of the Wigner function can be evaluated using Eq. (39). The Wigner functions for different values of p and t are shown in Figs. (1a), (1b), and (1c) on the left panel of Fig. 1. The Wigner function has both positive and negative values in different regions of phase space. The eigenfunctions and eigenvalues give a correct representation of the Wigner function as it depends only on the accuracy of the eigenvalues and eigenfunctions, and not on the accuracy of the method of propagating forward in time.

The non-stationary state we have used leads to an initial Wigner function with significant spatial and temporal variations as well as regions of negative values. These properties provide a stringent test of the methods of using Eqs. (19)-(21) or Eqs. (22)-(23) to propagate the Wigner function.

For our tests we take the initial Wigner function for our non-stationary state Eq. (44) at time $t = 0$, and evolve the Wigner function using the explicit solution. We carry out the time evolution using small time increments. We can choose either Eqs. (19)-(21) or Eqs. (22)-(23) to evolve the Wigner function. The former includes higher order effects in δt, and can be used with a larger time increment than the second approach. We choose to use Eqs. (19)-(21), and the results for the time evolution from $t = 0$ to $t = 3$ in Figs. (1a'), (1b'), and (1c') were calculated using 30 time steps. The cosine and sine transforms can be calculated using the method of fast Fourier transforms. The numerical integration over p_0 in Eq. (19) can then be carried out to yield the Wigner function at the next time step. This process is repeated in a stepwise manner to propagate forward in time. The resulting time evolution of the Wigner function is shown in Figs. (1a'), (1b'), and (1c') on the right panel of Fig. 1.

A comparison of the left and the right panels indicates that the explicit solution of Eqs. (19)-(21) gives an excellent reproduction of the time evolution of the Wigner

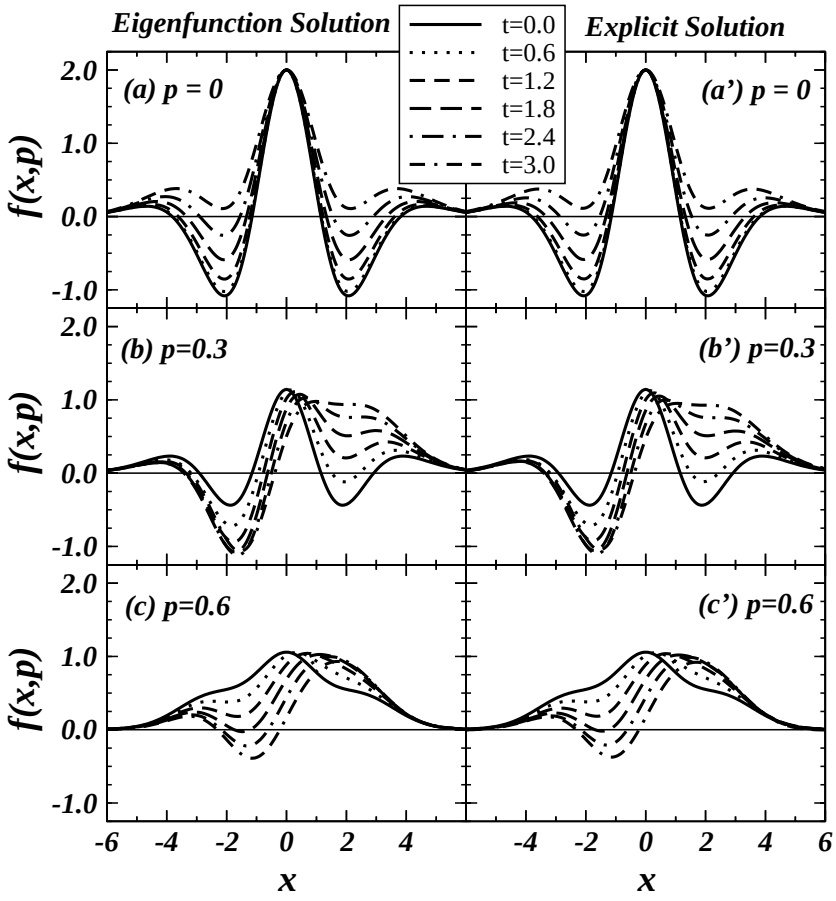

Figure 1. Time dependence of the Wigner function obtained in two different methods. The left panel gives the Wigner function obtained from eigenfunctions and eigenvalues, and the right panel shows that Wigner function obtained by the explicit solution of Eqs. (19)-(21).

function obtained by using eigenvalues and eigenfunctions. The phases and the negative regions of the Wigner function are correctly reproduced. The difference between the eigenfunction solution and the explicit solution is small. For example, for $p = 0.6$ at $t = 3$, the maximum value of the eigenfunction solution of the Wigner function is 0.9313 at $x = 1.692$, and the explicit solution gives 0.9206 at $x = 1.692$. For this momentum p and $t = 3$, the minimum of the eigenfunction solution of the Wigner function is -0.3888 at $x = -1.1667$, and the the explicit solution gives -0.3735 at $x = -1.1667$. The positions of the maxima and minima in the two methods are the same, and the magnitudes differ by about 1%. The explicit solution of Eqs. (19)-(21) thus leads to an accurate determination of the time evolution of the Wigner function, even if it contains regions of negative or oscillating values.

5. Pseudoparticle Method and Approximations

As an approximation to obtain the explicit solution of Eqs. (4), (10) and (11), a pseudoparticle method was presented previously to calculate the time evolution of the Wigner function [3]. It is useful to test the pseudoparticle method with our numerical example to assess its usefulness and accuracy.

To introduce the pseudoparticle method, we rewrite Eq. (17) in the form [3, 25]

$$f(\boldsymbol{rp},t)=\int d\boldsymbol{r}_0 d\boldsymbol{p}_0 \Delta(\boldsymbol{p}-\boldsymbol{p}_0+\nabla_r V(\boldsymbol{r},t)\delta t)\delta(\boldsymbol{r}-\boldsymbol{r}_0-\frac{\boldsymbol{p}}{m}\delta t)f(\boldsymbol{r}_0,\boldsymbol{p}_0,t_0), \tag{46}$$

where

$$\Delta(\boldsymbol{\pi})=\int \frac{d\boldsymbol{s}}{(2\pi\hbar)^3}\exp\left[i\left\{\frac{\boldsymbol{s}\cdot\boldsymbol{\pi}}{\hbar}+\frac{2\delta t}{\hbar}\sum_{n=1}^{\infty}\frac{1}{(2n+1)!}\left(\frac{\boldsymbol{s}\cdot\nabla_r^V}{2}\right)^{2n+1}V(\boldsymbol{r},t)\right\}\right], \tag{47}$$

and $\boldsymbol{\pi}=\boldsymbol{p}-\boldsymbol{p}_0+\nabla_r V(\boldsymbol{r},t)\delta t$. One notes that the second term in the exponential function is a sum involving third and higher powers of $\boldsymbol{s}$. If one neglects these higher-order terms in the exponential function, then one obtains the approximation

$$\Delta(\boldsymbol{p}-\boldsymbol{p}_0+\nabla_r V(\boldsymbol{r},t)\delta t)\approx\delta(\boldsymbol{p}-\boldsymbol{p}_0+\nabla_r V(\boldsymbol{r},t)\delta t) \tag{48}$$

and the time evolution of the Wigner function becomes [3]

$$f(\boldsymbol{rp},t)\approx f_{LO}(\boldsymbol{rp},t)=\int d\boldsymbol{r}_0 d\boldsymbol{p}_0 \delta(\boldsymbol{p}-\boldsymbol{p}_0+\nabla_r V(\boldsymbol{r},t)\delta t)\delta(\boldsymbol{r}-\boldsymbol{r}_0-\frac{\boldsymbol{p}}{m}\delta t)f(\boldsymbol{r}_0,\boldsymbol{p}_0,t_0), \tag{49}$$

which leads to

$$f(\boldsymbol{rp},t)\approx f_{LO}(\boldsymbol{rp},t)=f(\boldsymbol{r}-\boldsymbol{p}\delta t/m,\ \boldsymbol{p}+\nabla_r V(\boldsymbol{r},t)\delta t,\quad t_0). \tag{50}$$

The above equation provides the basis for the lowest-order (LO) pseudoparticle approximation of the time evolution of the Wigner function [3]. One divides the phase space into cells (pseudoparticles) and follows the trajectories of these pseudoparticles using classical equations of motion, Eqs. (12) and (13). Eq. (50) specifies that the Wigner function at the new phase space point $(\boldsymbol{rp})$ at $t=t_0+\delta t$ is approximately the same as the initial Wigner function at the initial classical trajectory phase space point $(\boldsymbol{r}-\boldsymbol{p}\delta t/m,\ \boldsymbol{p}+\nabla_r V(\boldsymbol{r},t)\delta t)$ at t_0. The subscript LO in $f_{LO}(\boldsymbol{rp},t)$ is to indicate that it is the solution of the lowest-order pseudoparticle approximation obtained by following classical trajectories. This method was used in [3] where it was found that the lowest-order pseudoparticle approximation reproduces quite well the general features of the time-dependent Hartree-Fock approximation. The use of classical trajectories to obtain an approximate time evolution of the Wigner function was also emphasized by Zachos and Curtright [14].

How good is the lowest-order pseudoparticle approximation? The accuracy of the pseudoparticle approximation depends on the potential $V(\boldsymbol{r},t)$. If the potential is a constant, a linear, or a harmonic oscillator potential, then even the LO pseudoparticle method gives the exact solution, as is clearly indicated in Eq. (47). The LO pseudoparticle solution deviates from the correct solution if the third and higher order spatial derivatives of the potential do not vanish.

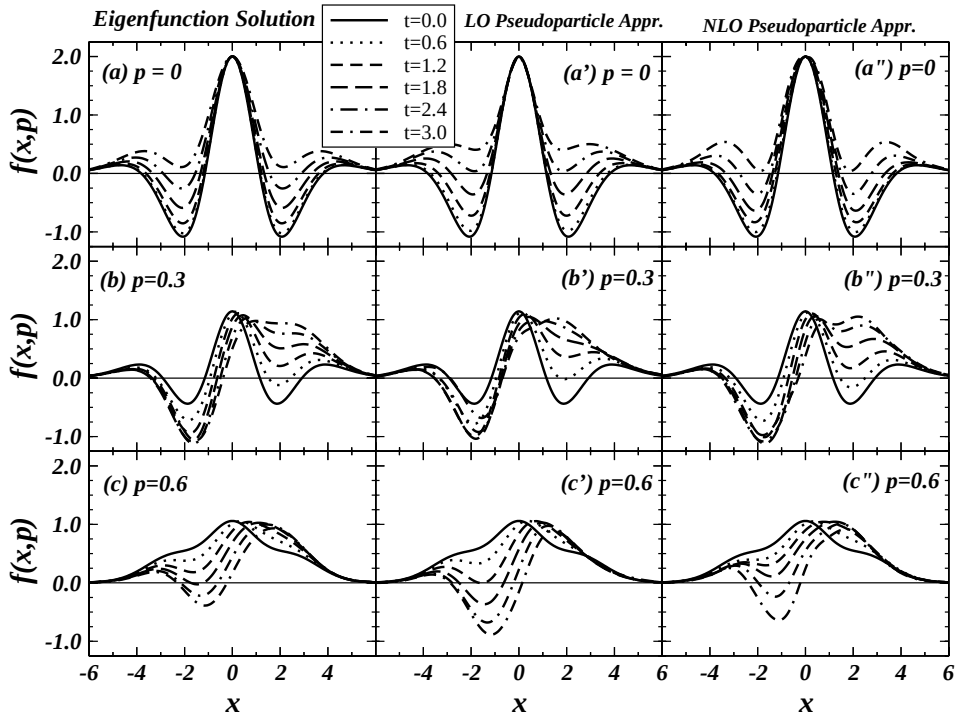

Figure 2. Time dependence of the Wigner function obtained in different methods. The left panel gives the correct Wigner function obtained from eigenfunctions and eigenvalues, the middle panel gives the results from the lowest-order (LO) pseudoparticle approximation, and the right panel shows the Wigner function obtained by the next-to-lowest (NLO) order pseudoparticle approximation with $\hbar^2$ corrections.

For the non-stationary state in a Gaussian potential in our test, we show the results of the LO pseudoparticle approximation in Figs. (2a'), (2b'), and (2c'), to be compared with the correct results from the eigenfunction method in Figs. (2a), (2b), and (2c). In our calculations, we specify the Wigner function at phase space coordinates of a fixed lattice. The Wigner function at the phase space points on the righthand side of Eq. (50) is obtained by interpolation using the Wigner function $f(\boldsymbol{r}_0, \boldsymbol{p}_0, t_0)$ at the earlier time t_0. As one observes, the general features of the oscillations are approximately reproduced. However, there are deviations from the correct results as time increases. For example, the Wigner function values for $p = 0$, $t = 3$, and $|x| \sim 2$ obtained in the LO pseudoparticle approximation in Fig. (2a') are much larger than the corresponding correct values in Fig. (2a). The values of the Wigner function for $p = 0.6$, $t = 3$, and $x \sim -1$ in the LO pseudoparticle approximation in Fig. (2c') are much smaller than the corresponding correct values in Fig. (2c).

We can correct for the deviations of the LO pseudoparticle approximation. For a small time increment δt, we can keep terms up to the first order in δt in Eq. (47). The function $\Delta(\boldsymbol{\pi})$ becomes

$$\Delta(\boldsymbol{\pi}) = \int \frac{d\boldsymbol{s}}{2\pi\hbar} e^{i\boldsymbol{s}\cdot\boldsymbol{\pi}/\hbar} \left[1 + \frac{2i\delta t}{\hbar} \sum_{n=1}^{\infty} \frac{1}{(2n+1)!} \left(\frac{\boldsymbol{s}\cdot\nabla_r^V}{2} \right)^{2n+1} V(\boldsymbol{r}, t) \right]. \tag{51}$$

The integration over $\boldsymbol{s}$ can be easily carried out and we obtain

$$\Delta(\boldsymbol{\pi}) = \left[1 + \delta t \sum_{n=1}^{\infty} \frac{1}{(2n+1)!} \left(\frac{\hbar}{2i}\right)^{2n} (\nabla_r^V \cdot \nabla_p^\delta)^{2n+1} V(\boldsymbol{r}, t)\right] \delta(\boldsymbol{\pi}), \tag{52}$$

where ∇_r^V acts on $V(\boldsymbol{r}, t)$ and ∇_p^δ acts on $\delta(\boldsymbol{\pi})$. The corrected pseudoparticle solution of the time evolution of the Wigner function is then

$$f(\boldsymbol{rp}, t) = \left[1 + \delta t \sum_{n=1}^{\infty} \frac{1}{(2n+1)!} \left(\frac{\hbar}{2i}\right)^{2n} (\nabla_r^V \cdot \nabla_p^f)^{2n+1} V(\boldsymbol{r}, t)\right] f_{LO}(\boldsymbol{r}, \boldsymbol{p}, t), \tag{53}$$

where ∇_p^f acts on $f_{LO}(\boldsymbol{r}, \boldsymbol{p}, t)$. It should be emphasized that no odd powers of $\hbar$ and even powers of $(\nabla_r^V \cdot \nabla_p^f)$ are present in the above expansion. We can improve upon the pseudoparticle approximation by including additional contributions in powers of $\hbar^2$ involving higher-order derivatives of $V(\boldsymbol{r}, t)$ and $f_{LO}(\boldsymbol{r}, \boldsymbol{p}, t)$.

We show in Figs. (2a"), (2b"), and (2c") the results in the next-to-lowest order approximation obtained by including the correction term of order $\hbar^2$, which involves the third derivatives of the potential and the Wigner function. In this calculation, we propagate the Wigner function from t_0 to $t = t_0 + \delta t$ for a small time increment δt following classical trajectories as in Eq. (49). The Wigner function is then corrected at time t using Eq. (53). The corrected Wigner function at t is used in Eq. (49) to propagate to time $t + \delta t$ by following classical trajectories. It is then corrected at time $t + \delta t$ using Eq. (53). These steps are repeated to obtain the time evolution of the Wigner function in this pseudoparticle approximation. To avoid numerical instability in the time evolution, we use the Wigner function $f_{LO}(\boldsymbol{rp}, t)$ obtained in the lowest-order approximation to calculate the third momentum derivative, when we evaluate the $\hbar^2$ correction term in Eq. (53).

Results in Fig. 2 indicate that the inclusion of the $\hbar^2$ correction term in the next-to-lowest (NLO) order improves the pseudoparticle approximation. In particular, the NLO values of the Wigner function at $p = 0$, $t = 3$, and $|x| \sim 2$ obtained with $\hbar^2$ corrections Fig. (2a") are now closer to the values obtained with eigenfunctions. The NLO values of the Wigner function at $p = 0.6$, $t = 3$, and $x \sim -1$ in Fig. (2c') are also closer to the corresponding values obtained with eigenfunctions. Although small deviations remain in the NLO solution, the general features of the Wigner function are reasonably well reproduced.

We give here an alternative method to evaluate the correction terms in the pseudoparticle method. As one notes in Eq. (52), the correction terms involve high-order derivatives of the δ-function. They can be evaluated approximately by expressing the δ-function in terms of known functions. Making use of the othonormality of the harmonic oscillator wave functions $\{\phi_m(x)\}$, we can represent a one-dimensional delta function $\delta(x)$ by

$$\delta(x) = \sum_{m=0}^{\infty} \phi_m^*(x)\phi_m(0) = \frac{\alpha}{\sqrt{\pi}} e^{-\frac{\alpha^2 x^2}{2}} \sum_{m=0}^{\infty} H_{2m}(\alpha x) \frac{(-1)^m}{2^{2m} m!}, \tag{54}$$

where $H_{2m}(\alpha x)$ is the Hermite polynomial of order $2m$, and α is a width parameter. In practice, the summation in the above equation is carried out up to an order M, and the

delta function $\delta(x)$ can be approximated by the distribution

$$\delta(x) \approx D(x) = A_M \frac{\alpha}{\sqrt{\pi}} e^{-\frac{\alpha^2 x^2}{2}} \sum_{m=0}^{M} H_{2m}(\alpha x) \frac{(-1)^m}{2^{2m} m!}, \tag{55}$$

where A_M is

$$A_M = \left[\sqrt{2} \sum_{m=0}^{M} (-1)^m \frac{(2m)!}{2^{2m} m! m!} \right]^{-1}, \tag{56}$$

and A_M is so chosen that $D(x)$ is normalized to $\int D(x)dx = 1$. A three-dimensional generalization of this D-function, $D(\boldsymbol{x})$, can be obtained as the product of three one-dimensional D-functions of their respective component coordinates, $D(x_x)D(x_y)D(x_z)$. Using a distribution function of this type, we can write the explicit solution of the Wigner function as

$$\begin{aligned} f(\boldsymbol{rp}, t) = f_{LO}(\boldsymbol{r}, \boldsymbol{p}, t) + \delta t \int d\boldsymbol{r}_0 d\boldsymbol{p}_0 \delta(\boldsymbol{r} - \boldsymbol{r}_0 - \frac{\boldsymbol{p}}{m}\delta t) f(\boldsymbol{r}_0, \boldsymbol{p}_0, t_0) \\ \times \sum_{n=1}^{\infty} \frac{1}{(2n+1)!} \left(\frac{\hbar}{2i} \right)^{2n} \left[(\nabla_r^V \cdot \nabla_p^D)^{2n+1} V(\boldsymbol{r}, t) D(\boldsymbol{p} - \boldsymbol{p}_0 + \delta t \nabla_r V(\boldsymbol{r}, t)) \right], \end{aligned} \tag{57}$$

where ∇_p^D applies to $D(\boldsymbol{p} - \boldsymbol{p}_0 + \delta t \nabla_r V(\boldsymbol{r}, t))$. As D is a known analytical function of $\boldsymbol{p}$, $(\nabla_p^D)^{2n+1} D(\boldsymbol{p} - \boldsymbol{p}_0 + \delta t \nabla_r V(\boldsymbol{r}, t))$ can be obtained analytically. The higher-order derivatives of the Wigner function in Eq. (53) can be converted into an integration over $\boldsymbol{p}_0$.

The pseudoparticle method utilizes classical trajectories and is easy to use. It is even exact for a constant, linear, or harmonic oscillator potential. The development of systematic higher-order corrections to the pseudoparticle method for a general potential in Eq. (53) allows one to improve on the approximate solution to make the pseudoparticle method a useful tool for future applications.

In applying the pseudoparticle method, one can use the Eulerian picture with a fixed lattice or alternatively the Lagrangian picture with a set of pseudoparticle phase space coordinates, as in molecular dynamics. The distribution D of Eq. (55) can be used to go from one picture to the other. For example, if one starts with a Wigner function in the Eulerian picture, one divides the phase space into pseudoparticle cells with volume element $\Delta\boldsymbol{r}_i \Delta\boldsymbol{p}_i$ and specifies the phase space coordinates $(\boldsymbol{r}_i \boldsymbol{p}_i)$ and its Wigner function $f(\boldsymbol{r}_i \boldsymbol{p}_i)$. The set of variables $(\boldsymbol{r}_i \boldsymbol{p}_i)$ and $f_L(\boldsymbol{r}_i \boldsymbol{p}_i)(= f(\boldsymbol{r}_i \boldsymbol{p}_i))$ can be used in the Lagrangian picture to evolve the phase space dynamics. Conversely, if one is given the set of variables $(\boldsymbol{r}_i \boldsymbol{p}_i)$ and $f_L(\boldsymbol{r}_i \boldsymbol{p}_i)$ in the Lagrangian picture, then the Wigner function in the Eulerian picture $f_E(\boldsymbol{rp})$ at coordinates $(\boldsymbol{rp})$ is given by

$$f_E(\boldsymbol{rp}) = \sum_i D_r(\boldsymbol{r} - \boldsymbol{r}_i) D_p(\boldsymbol{p} - \boldsymbol{p}_i) f_L(\boldsymbol{r}_i \boldsymbol{p}_i) \Delta\boldsymbol{r}_i \Delta\boldsymbol{p}_i, \tag{58}$$

where the width parameter α in D_r (and D_p) depends on the magnitude of $\Delta\boldsymbol{r}_i$ (and $\Delta\boldsymbol{p}_i$). These transcriptions between the two pictures facilitate the application of the pseudoparticle method.

6. Conclusions and Discussions

We have reviewed and applied here the explicit solution of the time evolution of the Wigner function obtained previously in 1982 [3]. The basic idea is to represent the Wigner function in terms of auxiliary phase space coordinates, which obey simple equations of motion. These equations are similar to the classical equations of motion. They can be solved easily. The solutions of these equations of motion can then be used to evaluate the time evolution of the Wigner function. We have demonstrated the usefulness of the explicit solution using a numerical example. We find that the explicit solution leads to the correct time evolution of the Wigner function, even for a Wigner function with strong spatial and temporal variations and regions of negative values.

We have also reviewed and tested the pseudoparticle method for the evaluation of the time evolution of the Wigner function. For our example of a non-stationary state in a Gaussian potential, the lowest-order pseudoparticle approximation gives the correct features of the time evolution, but there are deviations from the correct results. We have developed a systematic way to improve the pseudoparticle method involving correction terms in powers of $\hbar^2$ containing high-order derivatives of the potential and the Wigner function.

The simplicity of the different methods discussed here will facilitate their application to quantum dynamics in phase space. They can be used to study quantum particle dynamics in a time-dependent, multi-dimensional potential. They can also be applied to study the one-body Wigner function of a many-particle system in a time-dependent mean-field potential, as in [3]. With the addition of a collision term, they can be used to describe the dynamics of a quantum Boltzmann equation. The explicit solution of Eqs. (19)-(21) or (22)-(23) is probably best handled in a lattice of phase space points, as the sine and cosine transforms are simplest in such a lattice. On the other hand, the pseudoparticle method of Eqs. (49) and (53) can be investigated both in terms of pseudoparticle phase space coordinates in the Lagrangian picture or alternatively in a fixed lattice of phase space points in the Eulerian picture. The use of pseudoparticle coordinates may provide substantial saving of computer storage capacity when a significant fraction of the phase space is empty. Future research using these methods will allow us to explore further the richness of quantum dynamics in phase space, which Professor Wigner first pioneered for us.

Acknowledgments

The author would like to thank Drs. E. Pollak and P. G. Reinhard for helpful discussions and communications. This research was supported by the Division of Nuclear Physics, Department of Energy, under Contract No. DE-AC05-00OR22725 managed by UT-Battelle, LLC.

References

[1] E. P. Wigner, Phys. Rev. **40**, 749 (1932).

[2] ?. Janszky, Y. S. Kim, and M. A. Man'ko, *Wigner function and phase-space approach in quantum mechanics*, to be published in the Journal of Optics B: Quantum and Classical Optics, June 2003.

[3] C. Y. Wong, Phys. Rev. **C25**, 1460 (1982).

[4] D. T. Smithey *et al*. Phys. Rev. Lett. **70**, 1244 (1993).

[5] D. Leibfried *et al*., Phys. Phys. Rev. Lett. **77**, 4281 (1996).

[6] G. Breitenbach, S. Schiller, and J. Mlynek, Nature **387**, 471 (1997).

[7] Ch. Kurtsiefer, T. Pfau, and J. Mlynek, Nature **386**, 150 (1997).

[8] A. I. Lvovsky *et al*. Phys. Rev. Lett. **87**, 050402 (2001).

[9] P. Lougovski, E. Solano, Z. M. Zhang, H. Walther, H. Mack, and W. P. Schleich, quant-ph/0206083.

[10] S. John and E. A. Remler, Ann.of Phys. 180 (1987) 152.

[11] E. Prugovečki, Ann. Phys.(N.Y.) **10**, 102 (1978).

[12] K. Takahashi, Prog. Theor. Phys. Supplement, **98**, 109 (1989).

[13] S. Mancini, V. I. Man'ko, and P. Tombesi, Phys. Lett. **A213**, 1 (1996); for a review, see V. I. Man'ko, quant-ph/9902079.

[14] T. Curtright and C. K. Zachos, J. Phys. **A32**, 771 (1999); C. K. Zachos and T. Curtright, Prog. Theor. Phys. Suppl. **135**, 244 (1999).

[15] M. Levanda and V. Fleurov, J. Phys. : Condensed Matter **6**, 7889 (1994); M. Levanda and V. Fleurov, Ann. Phys. **292**, 199 (2001); M. Levanda and V. Fleurov, cond-mat/0111436.

[16] V. S. Filinov, J. Mol. Phys. **88**, 1517, 1529 (1996); V. Filinov, Yu. Lozovik, A. Filinov, I. Zacharov, and A. Oparin, Physica Scripta **58**, 304 (1998); V. S. Filinov, P. Thomas, I. Varga, T. Meier, M. Bonitz, V. Fortov, and S. Koch, Phys. Rev. **B65**, 165124 (2002), cond-mat/0203585.

[17] J. Ankerhold, M. Saltzer, and E. Pollak, J. Chem. Phys. **116 (14)**, 5925 (2002); J. L. Liao and E. Pollak, J. Chem. Phys. **116 (7)**, 2718 (2002); E. Pollak and J. S. Shao, J. Chem. Phys. **116 (4)**, 1748 (2002).

[18] L. Shifren and D. K. Ferry, Physica **B314**, 72 (2002).

[19] K. Morawetz, Phy. Rev. **E61**, 2555 (2000).

[20] A. N. Fedorova and M. G. Zeitlin, in Proceedings of the Capri ICFA Workshop, October, 2000, physics/0101006.

[21] H.-Th. Elze and U. Heinz, Phy. Rep. **183**, 81 (1989); H.-Th. Elze Nucl. Phys. **B436**, 213 (1995); H.-Th. Elze and J. Rafelski, and L. Turko, Phys. Lett. **B506**, 123 (2001).

[22] J. P. Blazoit and E. Iancu, Nucl. Phys. **B557**, 183 (1999).

[23] P.-G. Reinhard and E. Suraud, Ann. Phys. (N.Y.) **216**, 98 (1995).

[24] J. Schnack and H. Feldmeier, Nucl. Phys. **A601**, 181 (1996).

[25] Eqs. (2.12) and (2.13) in Ref. [3] correspond respectively to Eqs. (46) and (47) in this paper. There were inadvertent typographical errors in the former equations. In Eq. (2.12) of [3], $\nabla\mathcal{V}$ should read $\nabla\mathcal{V}\delta t$ and $f(\boldsymbol{r}_0, \boldsymbol{p}_0, t)$ should read $f(\boldsymbol{r}_0, \boldsymbol{p}_0, t_0)$, and in Eq. (2.13), the factor 1/6 should read $(1/6) \times (\delta t/4)$.